Assembly of Tobacco Mosaic Virus into Fibrous and Macroscopic Bundled Arrays Mediated by Surface Aniline Polymerization

ARTICLE *in* LANGMUIR · JULY 2007

Impact Factor: 4.46 · DOI: 10.1021/la070096b · Source: PubMed

Research Article

Assembly of Tobacco Mosaic Virus into Fibrous and Macroscopic Bundled Arrays Mediated by Surface Aniline Polymerization

Zhongwei Niu, Michael A. Bruckman, Siqi Li, L. Andrew Lee, Byeongdu Lee, Sai Venkatesh Pingali, P. Thiyagarajan, and Qian Wang

Langmuir, **2007**, 23 (12), 6719-6724 • DOI: 10.1021/la070096b

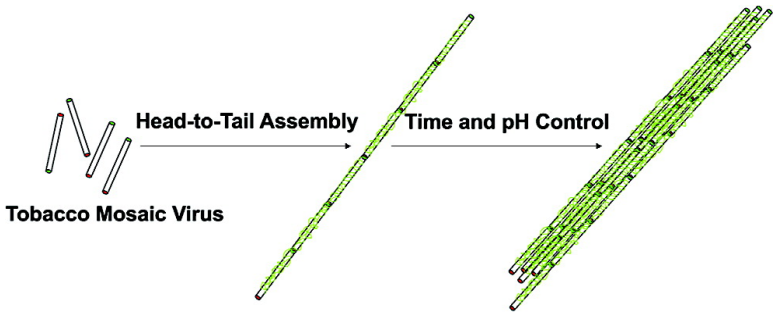

More About This Article

Additional resources and features associated with this article are available within the HTML version:

- Supporting Information
- Links to the 13 articles that cite this article, as of the time of this article download
- Access to high resolution figures
- Links to articles and content related to this article
- Copyright permission to reproduce figures and/or text from this article

View the Full Text HTML

Assembly of Tobacco Mosaic Virus into Fibrous and Macroscopic Bundled Arrays Mediated by Surface Aniline Polymerization

Zhongwei Niu,[†,||] Michael A. Bruckman,[†,||] Siqi Li,[†] L. Andrew Lee,[†] Byeongdu Lee,*[,‡] Sai Venkatesh Pingali,[§] P. Thiyagarajan,*[,§] and Qian Wang*[,†]

Department of Chemistry and Biochemistry and Nanocenter, University of South Carolina, 631 Sumter Street, Columbia, South Carolina 29208, Advanced Photon Source, Argonne National Laboratory, 9700 South Cass Avenue, Argonne, Illinois 60439, Intense Pulse Neutron Source, Argonne National Laboratory, 9700 South Cass Avenue, Argonne, Illinois 60439

Received January 12, 2007. In Final Form: March 7, 2007

One-dimensional (1D) polyaniline/tobacco mosaic virus (TMV) composite nanofibers and macroscopic bundles of such fibers were generated via a self-assembly process of TMV assisted by in-situ polymerization of polyaniline on the surface of TMV. At near-neutral reaction pH, branched polyaniline formed on the surface of TMV preventing lateral association. Therefore, long 1D nanofibers were observed with high aspect ratios and excellent processibility. At a lower pH, transmission electron microscopy (TEM) analysis revealed that initially long nanofibers were formed which resulted in bundled structures upon long-time reaction, presumably mediated by the hydrophobic interaction because of the polyaniline on the surface of TMV. In-situ time-resolved small-angle X-ray scattering study of TMV at different reaction conditions supported this mechanism. This novel strategy to assemble TMV into 1D and 3D supramolecular composites could be utilized in the fabrication of advanced materials for potential applications including electronics, optics, sensing, and biomedical engineering.

Introduction

Methods developed for controlling the supramolecular organization of macromolecular systems into hierarchical ordered structures are crucial for developing novel nanoscale optical, electronic, acoustic, and magnetic materials. Combination of biological elements into nanomaterial synthesis offers the possibility to generate highly ordered and programmable anisotropic structures for applications in material science and biomedicine.[1−4] Biological nanoparticles such as viruses, ferritin, and self-assembled protein complexes allow genetic programmability and site-specific chemistry at near-atomic scale, providing highly promising opportunities for the fabrication of nanoscale materials with novel functionalities.[5−11] Genetically engineered and chemically modified viruses have been used to direct material synthesis by controlling composition, mutation positions, and morphologies.[12−17] We are interested in the synthesis of nanofibers with large aspect ratios and tunable diameters by using the one-dimensional (1D) assembly of tobacco mosaic virus (TMV),[18] as 1D nanostructure fabrication is an emerging research area for advanced nanoelectronics and other applications.[19]

TMV, one of the earliest characterized viruses, consists of 2130 identical coat protein subunits assembled helically by wrapping around a single RNA strand. The rod-shaped virus is approximately 300 nm in length and 18 nm in diameter with a 4 nm interior channel. Figure 1 shows the transmission electron microscopy (TEM) image of wild-type TMV. The virion exhibits remarkable stability at temperatures up to 60 °C for hours and in a pH range 2−10.[20] Recent studies show that the surface properties of TMV can be manipulated chemically or genetically without disrupting the integrity and morphology of the capsids.[21,22] Nematic liquid crystalline phase formed by TMV at high concentrations was used as a template in the synthesis of mesostructured silica.[23] The polar outer and inner surfaces of TMV serve as a versatile platform to grow metal or metal oxide nanoparticles such as iron oxyhydroxides, CdS, PbS, gold, nickel,

* To whom correspondence should be addressed. E-mail: wang@mail.chem.sc.edu (Q.W.); blee@aps.anl.gov (B.L.); thiyaga@anl.gov (P.T.).
† University of South Carolina.
‡ Advanced Photon Source, Argonne National Laboratory.
§ Intense Pulse Neutron Source, Argonne National Laboratory.
|| These authors contributed equally to this work.

(1) Niemeyer, C. M. *Angew. Chem., Int. Ed.* **2001**, *40*, 4128.
(2) Dujardin, E.; Mann, S. *Adv. Eng. Mater.* **2002**, *4*, 461.
(3) Seeman, N. C. *Chem. Biol.* **2003**, *10*, 1151.
(4) Shih, W. M.; Quispe, J. D.; Joyce, G. F. *Nature* **2004**, *427*, 618.
(5) Flynn, C. E.; Lee, S.-W.; Peelle, B. R.; Belcher, A. M. *Acta Mater.* **2003**, *51*, 5867.
(6) Lee, L. A.; Wang, Q. *Nanomedicine* **2006**, *2*, 137.
(7) Raja, K. S.; Wang, Q. *Encycl. Nanosci. Nanotechnol.* **2004**, *B*, 321.
(8) Wong, K. K. W.; Douglas, T.; Gider, S.; Awschalom, D. D.; Mann, S. *Chem. Mater.* **1998**, *10*, 279.
(9) Meldrum, F. C.; Douglas, T.; Levi, S.; Arosio, P.; Mann, S. *J. Inorg. Biochem.* **1995**, *58*, 59.
(10) Douglas, T.; Stark, V. T. *Inorg. Chem.* **2000**, *39*, 1828.
(11) Lin, Y.; Boker, A.; He, J.; Sill, K.; Xiang, H.; Abetz, C.; Li, X.; Wang, J.; Emrick, T.; Long, S.; Wang, Q.; Balazs, A.; Russell, T. P. *Nature* **2005**, *434*, 55.
(12) Lee, S.-W.; Mao, C.; Flynn, C. E.; Belcher, A. M. *Science* **2002**, *296*, 892.
(13) Douglas, T.; Young, M. *Nature* **1998**, *393*, 152.
(14) Wang, Q.; Lin, T.; Tang, L.; Johnson, J. E.; Finn, M. G. *Angew. Chem., Int. Ed.* **2002**, *41*, 459.
(15) Douglas, T.; Young, M. *Science* **2006**, *312*, 873.
(16) Mao, C.; Solis, D. J.; Reiss, B. D.; Kottmann, S. T.; Sweeney, R. Y.; Hayhurst, A.; Georgiou, G.; Iverson, B.; Belcher, A. M. *Science* **2004**, *303*, 213.
(17) Nam, K. T.; Kim, D. W.; Yoo, P. J.; Chiang, C. Y.; Meethong, N.; Hammond, P. T.; Chiang, Y. M.; Belcher, A. M. *Science* **2006**, *312*, 885.
(18) Niu, Z.; Bruckman, M. A.; Kotakadi, V. S.; He, J.; Emrick, T.; Russell, T. P.; Yang, L.; Wang, Q. *Chem. Commun.* **2006**, 3019.
(19) Selected references: (a) Huang, Y.; Duan, X.; Wei, Q.; Lieber, C. M. *Science* **2001**, *291*, 630. (b) Baughman, R. H.; Zakhidov, A. A.; de Heer, W. A. *Science* **2002**, *297*, 787. (c) Cui, Y.; Lieber, C. M. *Science* **2001**, *291*, 851. (d) Melosh, N. A.; Boukai, A.; Diana, F.; Gerardot, B.; Badolato, A.; Petroff, P. M.; Heath, J. R. *Science* **2003**, *300*, 112.
(20) Shenton, W.; Douglas, T.; Young, M.; Stubbs, G.; Mann, S. *Adv. Mater.* **1999**, *11*, 253.
(21) Schlick, T. L.; Ding, Z.; Kovacs, E. W.; Francis, M. B. *J. Am. Chem. Soc.* **2005**, *127*, 3718.
(22) Yi, H.; Nisar, S.; Lee, S. Y.; Powers, M. A.; Bentley, W. E.; Payne, G. F.; Ghodssi, R.; Rubloff, G. W.; Harris, M. T.; Culver, J. N. *Nano Lett.* **2005**, *5*, 1931.
(23) Fowler, C. E.; Shenton, W.; Stubbs, G.; Mann, S. *Adv. Mater.* **2001**, *13*, 1266.

10.1021/la070096b CCC: $37.00
Published on Web 05/03/2007

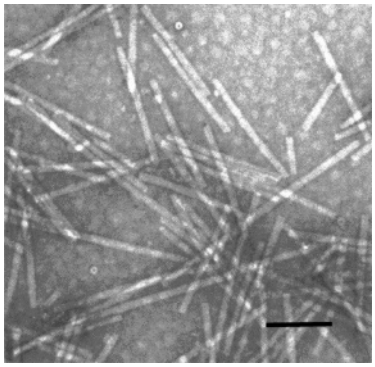

Figure 1. TEM image of wild-type TMV. (The scale bar is 150 nm.)

cobalt, silver, copper, and iron oxides.[20,23−31] The nanofibers formed by the 1D head-to-tail assembly have already shown great potential in the nanoelectronics applications.[32,33] In this paper, we report the synthesis and the mechanism of formation of 1D and 3D organization of TMV as functions of TMV concentration, surface polyaniline content, and reaction pH. Small-angle X-ray scattering (SAXS) was used to characterize the polymerization reaction on TMV surfaces.

Experimental Section

Purification of TMV. TMV was obtained from tobacco plants. Tobacco plants approximately 1 month old were inoculated with TMV. The leaves were harvested and the virus was isolated from the host plant. The leaves were crushed and added to 0.01 M potassium phosphate buffer at pH 7.8 with 0.2% β-mercaptoethanol. The mixture was centrifuged at 9000 rpm for 15 min before the supernatant was treated with a 1:1 ratio of $CHCl_3$:1-butanol. The aqueous portion was separated and TMV was precipitated by the addition of polyethylene glycol 8 K and NaCl. The resultant pellets were resuspended in 0.01 M potassium phosphate buffer at pH 7.8. After a final ultracentrifugation at 42 000 rpm for 2.5 h, pure TMV obtained was resuspended overnight in 0.01 M potassium-phosphate buffer at pH 7.8 or in pure water.

Synthesis of Polyaniline/TMV Composites. In a typical synthesis, distilled aniline (10 μL) and 10 mg/mL of ammonium persulfate (1 mL) were added to a 1 mg/mL solution of TMV (4 mL) in succession. The solutions of 0.1 M HCl aq and 0.1 M NaOH aq were used to adjust the pH. The reaction mixture was incubated at room temperature for 24 h. Later, the reaction mixture was centrifuged at 9500 rpm for 15 min. After centrifugation, the pellet was immediately rinsed three times with pure water before resuspending in deionized water to obtain pure polyaniline/TMV composite nanofibers.

Analysis and Characterization. A 0.2 mg/mL TMV or polyaniline/TMV composite nanofiber solution (20 μL) was deposited onto a 300-mesh carbon-coated copper grid for 2 min. The grid was then stained with 20 μL of 2% uranyl acetate and was characterized with a JEOX 100 CX II transmission electron microscope. Tapping-mode atomic force microscopy (AFM) images were obtained at ambient conditions using a NanoScope IIIA MultiMode AFM (Veeco). Si tips with a resonance frequency of approximately 300 kHz, a spring constant of about 40 N m^{-1}, and a scan rate of 0.5 Hz were used. SAXS and TRSAXS of solutions were measured at Sector 12, Advanced Photon Source in Argonne National Laboratory. X-ray beam of energy 16 keV and a ca. 4 mm thick solution sample cell with mica windows were used. UV−vis absorption studies were performed using an Agilent 8453 UV−vis spectrometer.

Results and Discussion

The rodlike TMV consists of regular helical arrangement of $16^1/_3$ identical protein capsids per turn. The length of the encapsulated RNA that assists and stabilizes the coat protein assembly of the native TMV is 300 nm (Figure 1).[34−36] Theoretically, TMV (or TMV coat proteins) can assemble head-to-tail endlessly in solution at suitable pH and ionic conditions because the surface morphology of each turn of the virus helix is identical.[35,37] However, TMV forms a nematic liquid crystalline phase at high concentrations resulting from the competition between rotational and translational entropy.[38,39] Therefore, to generate stable long 1D nanofibers, surface coating was used to favor head-to-tail assembly (pathway A**)** thereby preventing the lateral association of individual TMV (pathway B) summarized in Figure 2.

Polyaniline was used as the surface-coating polymer for its intrinsic anisotropic morphology, the ease with which aniline polymerizes in aqueous solutions, and its conductive properties.[40] At near-neutral reaction pH, long one-dimensional polyaniline-coated TMV single nanofibers formed upon treating TMV with a dilute solution of aniline and ammonium persulfate (APS) (Figure 2**;** pathway A).[18] Polymerization of aniline on TMV surface was the key for the formation of long 1D head-to-tail assembly of TMV nanofibers. The formation of highly branched polyaniline at near-neutral reaction pH prevents lateral association of single polyaniline/TMV nanofibers because of an increase in steric repulsion.[41,42] Therefore, polyaniline/TMV nanofibers could be dispersed readily in water and also on a mica surface (Figure 3b). This behavior is quite different from that of the wild-type TMV which shows pronounced lateral association (Figure 3a).[43,44] As discussed in our earlier paper, the fibers exhibited fairly homogeneous diameter and high aspect ratio.[18] However, the nanofibers produced at near-neutral reaction pH were not conductive that might be due to the branched structures of polyaniline.

Polymerization reactions were performed in acidic conditions to understand the formation of conductive nanofibers. At low reaction pH of 2.5 and 3.9, green polyaniline/TMV composites were observed after a 24 h reaction at room temperature indicating the formation of the emeraldine form of polyaniline.[45,46] The color of the reaction mixture changed from dark yellow at reaction

(24) Royston, E.; Lee, S. Y.; Culver, J. N.; Harris, M. T. *J. Colloid Interface Sci.* **2006**, *298*, 706.
(25) Fonoberov, V. A.; Balandin, A. A. *Nano Lett.* **2005**, *5*, 1920.
(26) Knez, M.; Kadri, A.; Wege, C.; Gosele, U.; Jeske, H.; Nielsch, K. *Nano Lett.* **2006**, *6*, 1172.
(27) Knez, M.; Bittner, A. M.; Boes, F.; Wege, C.; Jeske, H.; Maiss, E.; Kern, K. *Nano Lett.* **2003**, *3*, 1079.
(28) Knez, M.; Sumser, M.; Bittner, A. M.; Wege, C.; Jeske, H.; Martin, T. P.; Kern, K. *Adv. Funct. Mater.* **2004**, *14*, 116.
(29) Knez, M.; Sumser, M. P.; Bittner, A. M.; Wege, C.; Jeske, H.; Hoffmann, D. M.; Kuhnke, K.; Kern, K. *Langmuir* **2004**, *20*, 441.
(30) Lee, S. Y.; Culver, J. N.; Harris, M. T. *J. Colloid Interface Sci.* **2006**, *297*, 554.
(31) Liu, W. L.; Alim, K.; Balandin, A. A.; Mathews, D. M.; Dodds, J. A. *Appl. Phys. Lett.* **2005**, *86*, 253108.
(32) Tseng, R. J.; Tsai, C.; Ma, L.; Ouyang, J.; Ozkan, C. S.; Yang, Y. *Nat. Nanotechnol.* **2006**, *1*, 72.
(33) Kalinin, S. V.; Jesse, S.; Liu, W. L.; Balandin, A. A. *Appl. Phys. Lett.* **2006**, *88*, 153902.
(34) Butler, P. J. G.; Lomonossoff, G. P. *J. Mol. Biol.* **1978**, *126*, 877.
(35) Butler, P. J. G. *Philos. Trans. R. Soc. London, Ser. B: Biol. Sci.* **1999**, *354*, 537.
(36) Butler, P. J. G.; Lomonossoff, G. P. *Biophys. J.* **1980**, *32*, 295.
(37) Klug, A. *Philos. Trans. R. Soc. London, Ser. B: Biol. Sci.* **1999**, *354*, 531.
(38) Dogic, Z.; Fraden, S. *Curr. Opin. Colloid Interface Sci.* **2006**, *11*, 47.
(39) Onsager, L. *Ann. N.Y. Acad. Sci.* **1949**, *51*, 627.
(40) Huang, J.; Kaner, R. B. *Chem. Commun.* **2006**, 367.
(41) Samuelson, L. A.; Anagnostopoulos, A.; Alva, K. S.; Kumar, J.; Tripathy, S. K. *Macromolecules* **1998**, *31*, 4376.
(42) Bloor, D.; Monkman, A. *Synth. Met.* **1987**, *21*, 175.
(43) Maeda, H. *Langmuir* **1997**, *13*, 4150.
(44) Wadu-Mesthrige, K.; Pati, B.; McClain, W. M.; Liu, G.-Y. *Langmuir* **1996**, *12*, 3511.
(45) Macdiarmid, A. G.; Chiang, J. C.; Richter, A. F.; Epstein, A. J. *Synth. Met.* **1987**, *18*, 285.

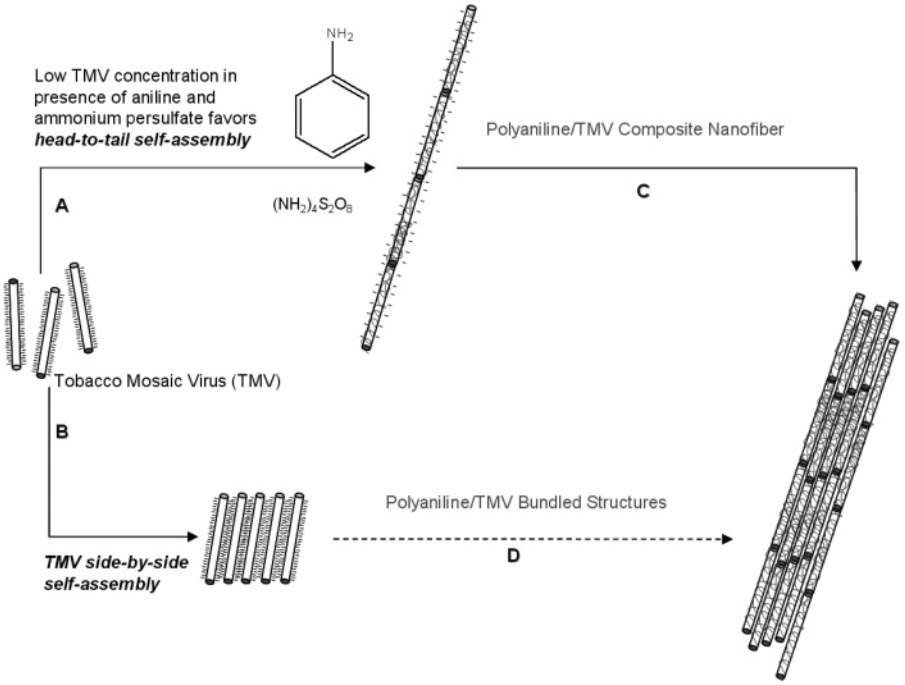

Figure 2. Schematic illustration of polyaniline/TMV composite nanofiber and bundled structure formation. (A) TMV head-to-tail assembly assisted by the polymerization of aniline on TMV surface to form long 1D nanofibers at low concentrations for low and near-neutral reaction pH; (B) TMV side-to-side assembly observed at high concentrations; and (C, D) Plausible mechanisms for the formation of polyaniline coated TMV bundled structures.

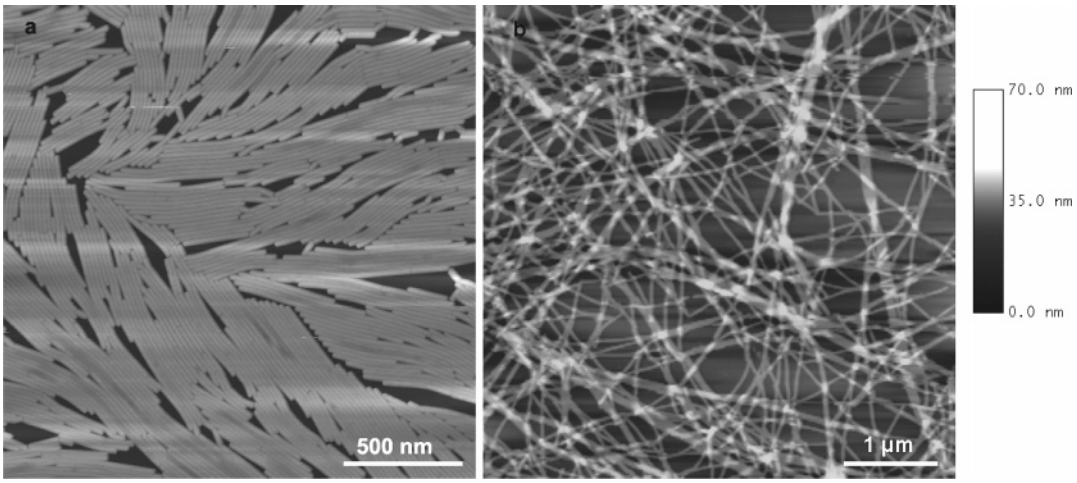

Figure 3. AFM height images: (a) wild-type TMV; (b) polyaniline/TMV composite fibers on a mica surface (dried at room temperature).

pH = 5.0 to bright yellow at reaction pH = 7.0. We attribute the color change to the formation of branched polyaniline or oligomers at near-neutral reaction pH.[41,42] Figure 4 shows the UV−vis spectra of polyaniline/TMV composite nanofibers synthesized at two different reaction conditions: pH = 2.5 (Figure 4a) and 7.0 (Figure 4b) as a function of solvent pH. These pH dependent experiments were done on samples after a reaction time of about 24 h. For the sample prepared at a reaction pH 2.5, three absorption peaks were observed at ca. 340, 440, and 850 nm (free carrier tail) for solvent pH of 1.0 (dark grey) and 4.0 (dotted line), suggesting an acid-doping state of polyaniline. The strong absorption peaks at ca. 340 and 650 nm observed at solvent pH 7.0 (grey) and 10.0 (light grey) were attributed to the formation of the emeraldine base state of polyaniline.[47,48] On the other hand, samples prepared at a reaction pH 7.0 showed no prominent change in the spectra when the solvent pH was varied from 1 to 10. This observation is consistent with the formation of highly branched polyaniline at near-neutral reaction pH.[42]

TEM images of polyaniline/TMV composite nanofibers shown in Figure 5 were synthesized at various reaction pH conditions. All these reactions were carried out for 24 h. At a reaction pH of 2.5, only short polyaniline/TMV composite nanofibers with a diameter of about 40 nm were detected (Figure 5a). At a higher reaction pH 5.0, bundled structures of nanofibers with lengths of several micrometers and widths of 1−2 micrometers were observed (Figure 5b). Figure 5c, an enlarged image of Figure 5b, shows that the bundle consists of parallel arrays of nanofibers. Similar structures were observed for samples synthesized at reaction pH 4.0 and 5.5 (data not shown). Figure 5d shows long 1D composite nanofibers formed at near-neutral reaction pH

(46) Epstein, A. J.; Ginder, J. M.; Zuo, F.; Bigelow, R. W.; Woo, H.-S.; Tanner, D. B.; Richter, A. F.; Huang, W.-S.; MacDiarmid, A. G. *Synth. Met.* **1987**, *18*, 303.

(47) Chiou, N. R.; Epstein, A. J. *Adv. Mater.* **2005**, *17*, 1679.

(48) Zhang, X.; Goux, W. J.; Manohar, S. K. *J. Am. Chem. Soc.* **2004**, *126*, 4502.

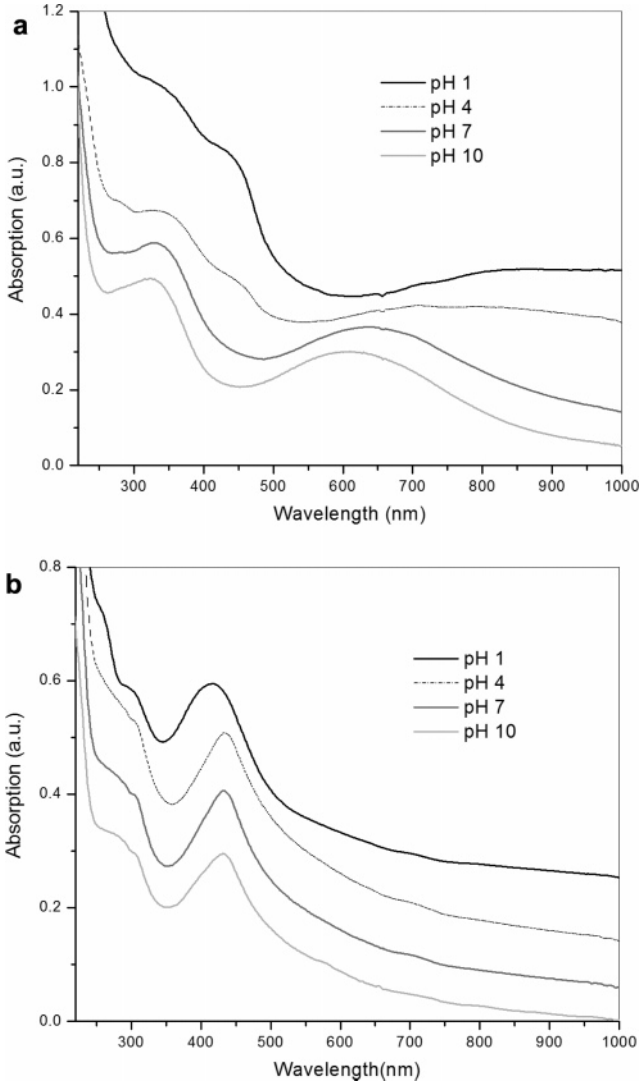

Figure 4. UV−vis spectra of polyaniline/TMV composite nanofibers synthesized at reaction pH (a) 2.5 and (b) 7.0. Reaction was carried out for 24 h prior to the preparation of samples at different solvent pH (1, 4, 7, and 10) for UV−vis spectroscopy experiments.

(=6.5) as in our earlier report.[18] At this reaction pH, since polyaniline exists as a branched polymer the lateral association of the fibers was prevented.

There are two possible pathways that could lead to the formation of bundled arrays at low reaction pH. (1) TMV organizes laterally prior to the initiation of the aniline polymerization resulting in bundles (pathway BD in Figure 2). (2) First, TMV assembles into long fibers through head-to-tail association followed by the aniline polymerization on the surface. The hydrophobic interaction mediated by the polyaniline on the surface of TMV nanofibers causes them to coalesce into bundles (pathway AC in Figure 2). In our view, the latter pathway is more plausible because the reactions were performed at low virus concentrations where TMVs remain as individual particles. A series of time-dependent studies were performed at a reaction pH 5.0 to confirm the plausible mechanism. TEM images of the morphologies at different time points of the reaction are summarized in Figure 6. After a reaction time of 30 min (Figure 6a), only short single nanofibers were observed. After 1 and 2 h (Figure 6b and 6c, respectively), a higher population of long single nanofibers and a hint of long bundled nanofibers were seen. However, after 4 h (Figure 6d) and beyond (data not shown), only bundled structures were observed. The progress from single short nanofibers to long

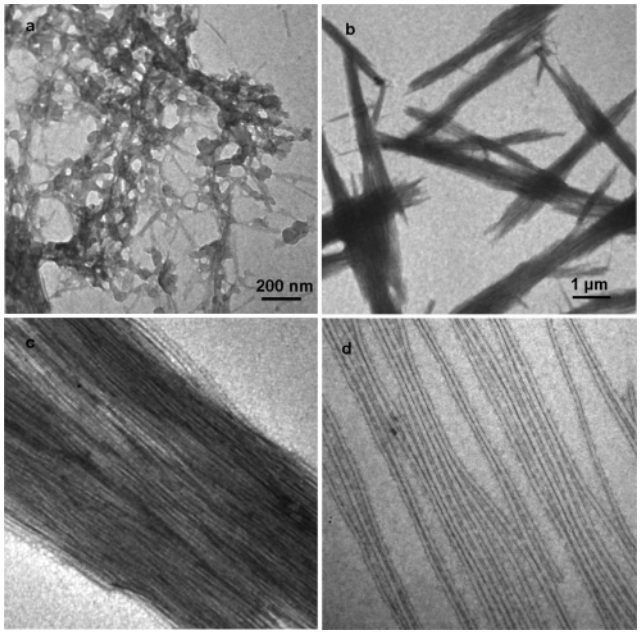

Figure 5. TEM images of polyaniline/TMV composites synthesized after a 24 h reaction at (a) pH 2.5, (b, c) pH 5.0, and (d) pH 6.5. Scale bar same for a, c, and d.

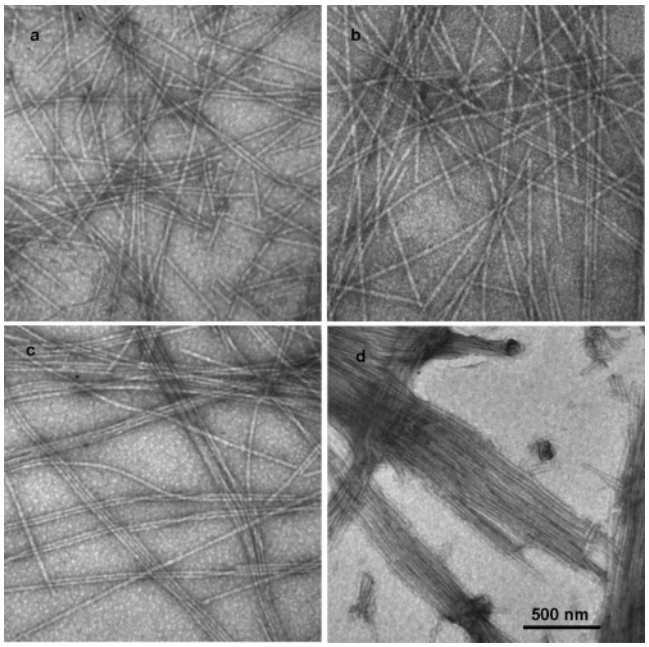

Figure 6. TEM images of the synthesis of polyaniline-coated TMV (reaction pH 5.0) at various time points of the reaction: (a) 30 min, (b) 1 h, (c) 2 h, and (d) 4 h.

nanofibers is attributed to the head-to-tail assembly of TMV subunits (pathway A in Figure 2).

By combining electron microscopy (EM) and AFM, the length and surface morphology of TMV and composite fibers can be readily investigated. However, samples prepared on substrates for EM and AFM characterization upon drying can potentially alter both the diameter and the surface morphology because of the interaction between the surface proteins and the substrate. As a complement to the TEM data, SAXS and in-situ time-resolved SAXS (TRSAXS) on solution samples were performed to understand the kinetics of polyaniline/TMV composite

(49) Glatter, O.; Kratky, O. *Small Angle X-ray Scattering*; Academic Press: London, 1982.

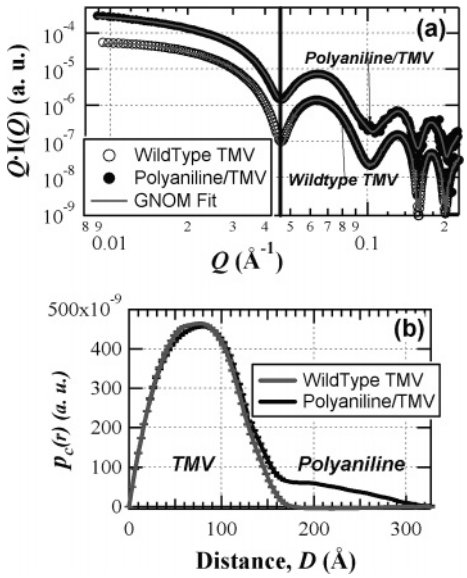

Figure 7. (a) SAXS data (dots) and fits using GNOM (gray solid line) for wild-type TMV (open circles) and polyaniline/TMV (black dots) in 0.01 M pH 7.8 K-phosphate. The top curve has been scaled for clarity. (b) Fitted pair distance distribution function (PDDF) as a function of radial distance from center of the wild-type TMV (gray solid line) and polyaniline/TMV (black solid line) obtained by fitting the SAXS data using GNOM. Wild-type TMV: 5 mg/mL. Polyaniline/TMV: 1 mg/mL and synthesized from a reaction of pH 6.5.

nanofiber formation. To illustrate the ability of SAXS to measure the growth of polyaniline on the TMV surface, we measured the SAXS of wild-type TMV and polyaniline/TMV after completion of the reaction. The difference in cross-sectional structure between wild-type TMV and polyaniline/TMV revealed by SAXS is shown in Figure 7.

The SAXS intensity curve for an infinitely long rodlike particle will exhibit a Q^{-1} power law at $Q \gg 1/Rg$. For rodlike particles, SAXS can be used to probe the cross-sectional structural information by using $Q \cdot I(Q)$ as the scattering intensity. The pair distance distribution function (PDDF) of the cross section of TMV, $p_c(r)$ is related to the total scattered intensity $I(Q)$ through eq 1.[49]

$$I(Q) = 2\pi^2 L \int_0^\infty p_c(r) \cdot \frac{J_0(Qr)}{Q} \, dr = I_c(Q) \cdot \frac{\pi \cdot L}{Q} \qquad (1)$$

where $J_0(Qr)$ is the zero-order Bessel function, L is the length of the cylinder, and $I_c(Q)$ is the scattering intensity of the cross-sectional structure. Through an inverse Fourier transform of $I_c(Q)$, the PDDF of the cross section can be obtained

$$p_c(r) = \frac{1}{2\pi} \int_0^\infty I_c(Q) \cdot (Qr) \cdot J_0(Qr) dr \qquad (2)$$

by using the software tool GNOM.[51,52]

The log−log plot of $I_c(Q)[Q \cdot I(Q)]$ versus Q in Figure 7a shows that scattering patterns for both wild-type TMV (open circles) and polyaniline/TMV (black dots) are similar in the range $Q > 0.02$ Å^{-1}. Good fits to the data were obtained using GNOM, and the corresponding PDDF curves are shown in Figure 7b. The largest dimension along the cross section (D) obtained for TMV is ~18 nm which is consistent with the TMV crystal structure.

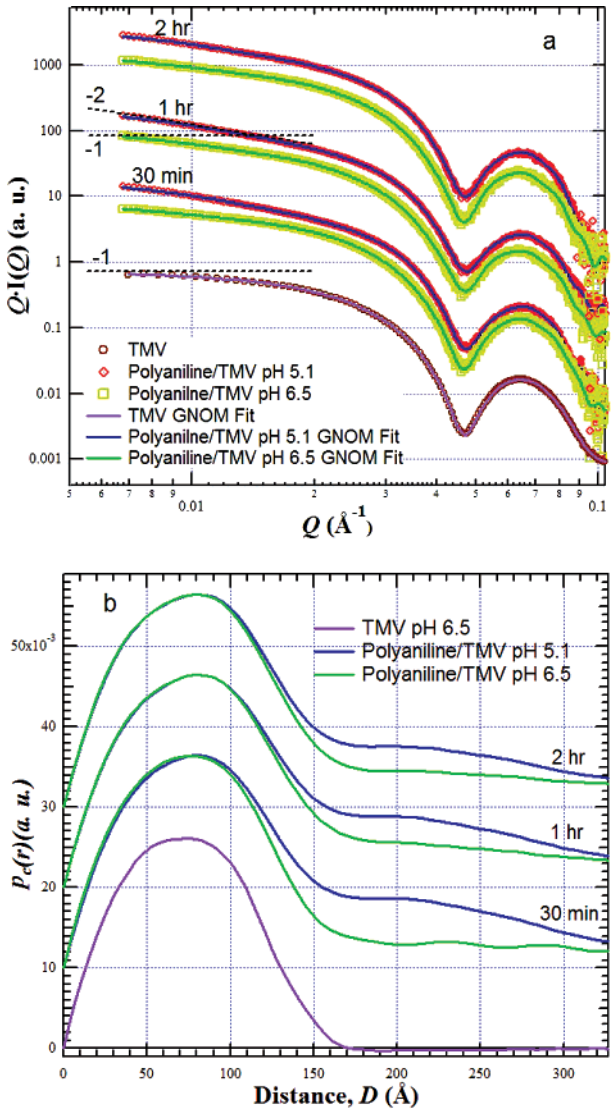

Figure 8. (a) In-situ TRSAXS was measured for wild-type TMV (brown circles) and polyaniline/TMV at reaction pH 5.1 (red open diamonds) and 6.5 (yellow open squares) at 2 h, 1 h, and 30 min. Solid lines are the GNOM fits wild type (lilac) and polyaniline/TMV at reaction pH 5.1 (blue) and 6.5 (green). (b) Fitted PDDF as a function of radial distance from the center of TMV (lilac solid line) and polyaniline/TMV (1 mg/mL) at reaction pH 5.1 (blue solid line) and 6.5 (green solid line). The curves for different reaction instants in all the figures were scaled for clarity. The power-law exponents of 1 and 2 were displayed as asymptotic dash lines.

For the polyaniline/TMV, the maximum cross-sectional dimension is 30 nm, and this increase in length scale can be attributed to the polyaniline coating of TMV.

To further explore the rate of polyaniline growth on TMV surface, in-situ TRSAXS was performed at two different reaction pH conditions (Figure 8). Similar to Figure 7a, it can be seen in Figure 8a that at all conditions the shape of the SAXS patterns for $Q > 0.02$ Å^{-1} is similar with a broad peak centered at $Q \sim 0.065$ Å^{-1} which is due to the hollow cylindrical structure of TMV. However, the scattering patterns vary in the low Q region ($Q < 0.01$ Å^{-1}) as a function of reaction pH and reaction time. In the case of TMV, the SAXS pattern exhibits a Q^{-1} power law expected for a long rod. However, the SAXS patterns for the TMV/polyaniline exhibit power-law exponents in the range of 1−2 depending on the reaction pH and the reaction time. The time-resolved $I_c(Q)$ data have been fitted using GNOM which produced the PDDF curves.

(50) Svergun, D. I. *J. Appl. Crystallogr.* **1991**, *24*, 485.
(51) Svergun, D. I. *J. Appl. Crystallogr.* **1992**, *25*, 495.
(52) Zhang, X.; Manohar, S. K. *Chem. Commun.* **2004**, 2360.

The PDDF curves in Figure 8b indicate that the polyaniline content on TMV surface for the two samples at reaction pH 5.1 and 6.5 is different. At a reaction pH 5.1, the rate of growth of polyaniline on TMV surface was higher and the reaction seemed to reach completion in 30 min. Furthermore, the higher PDDF values in 18−30 nm length scale may likely be due to the linear growth of the polymer at this reaction condition. At a reaction pH 6.5, the rate of polyaniline growth seems to be slower as it took 2 h to attain equilibrium. Even after 2 h of reaction time, the length of the polyaniline on TMV surface was smaller than that at the reaction pH 5.1, and this could be due to the branching during polymerization at higher reaction pH.

For the experimental conditions used in the SAXS experiments, we did not observe any ordered bundling of the nanofibers of TMV. If the nanofibers with a cross-sectional diameter of 30 nm would associate as hexagonal packed cylinders, diffraction peaks would occur around $Q \sim 0.021$, 0.036, and 0.042 $Å^{-1}$ convoluted with the form factor for the hollow cylinder structure of the TMV. In-situ TRSAXS studies are underway to investigate the detailed thermodynamics of the formation of laterally associated arrays of polyaniline coated TMV (pathway AC in Figure 2) as a function of concentration, temperature, pH, and ionic conditions, and the results will be reported elsewhere.

Evidently, TEM and SAXS show that polyaniline, by preventing lateral association, assists TMV in its head-to-tail assembly at near-neutral reaction pH. TRSAXS showed that the polymerization was fast at a low reaction pH and likely formed the linear, para-directed polyaniline on TMV surface. The process of polyaniline formation on TMV surface is most probably favored by the electrostatic interaction (or hydrogen bonding) between TMV and polyaniline. The surface charge of polyaniline/TMV nanofibers progressively reduces with the reaction time because of the accumulation of polyaniline on the surface. Hydrophobic interaction between the polyaniline molecules on TMV surfaces and the competition between rotational and translational entropy drove the formation of bundles as observed by TEM. At near-neutral reaction pH, the polymerization was slow and only branched (ortho-para directed) structures of polyaniline were formed that also prohibited the formation of bundled structures because of steric repulsion.

We also measured the DC conductivity of the thin films formed at different reaction pH. Thin films were prepared by depositing a suspension of polyaniline/TMV composite nanofibers on a glass slide and were dried. At room temperature, the bulk DC conductivities measured were in the range of 0.01−0.1 S cm^{-1} for composite nanofibers synthesized at low reaction pH (2.5 and 4.0). Standard four-probe method was used for these measurements. This is comparable to the polyaniline nanofibers synthesized by other methods.[41,47,48,52,53] No conductivity was observed for the composite nanofibers formed at a higher reaction pH.

Conclusion

In summary, 1D polyaniline/TMV composite nanofibers were synthesized by the head-to-tail self-assembly of rodlike TMV, assisted by the polyaniline synthesized on the TMV surface at various reaction pH conditions. At near-neutral reaction pH, the long nanofibers formed have homogeneous diameter, high aspect ratio, and good processibility. At low reaction pH, mostly bundled structures were obtained. Time-dependent TEM studies showed that initially long fibers form at low reaction pH. After 4 h of reaction, accumulation of excess polyaniline on the nanofiber surface leads to the formation of bundled structures mediated by the hydrophobic interaction because of polyaniline on the surface of the nanofibers. SAXS established the presence of polyaniline on the exterior surface of TMV. The head-to-tail TMV assembly for the single nanofiber formation is consistent with TR-SAXS studies although, because of dilute TMV solutions, bundled structures were not observed. We have demonstrated a unique way to assemble TMV into different nanoscopically ordered macroscopic structures that may have potential applications in electronics, optics, sensing, and biomedical engineering.

Acknowledgment. The work was partially supported by the U.S. ARO-MURI program, DoD-DURIP, and the W. M. Keck Foundation. This work benefited from the use of 12-ID at APS and from the IPNS, funded by U.S. DOE-BES under contract # DE-AC02-06CH11357.

LA070096B

(53) Huang, J.; Kaner, R. B. *Chem. Commun.* **2006**, 367.